PERGAMON

International Journal of Heat and Mass Transfer 44 (2001) 1153–1159

International Journal of HEAT and MASS TRANSFER

www.elsevier.com/locate/ijhmt

A numerical study of interfacial convective heat transfer coefficient in two-energy equation model for convection in porous media

Fujio Kuwahara, Mitsuhiro Shirota, Akira Nakayama *

Department of Mechanical Engineering, Shizuoka University, 3-5-1 Johoku, Hamamatsu 432, Japan

Received 12 January 2000; received in revised form 28 April 2000

Abstract

A numerical experiment has been conducted to determine the interfacial convective heat transfer coefficient in the two-energy equation model for convection in porous media, which is needed when the local thermal equilibrium between the fluid and solid phases breaks down. The similarity of periodically fully developed temperature profiles allows one to perform a numerical experiment using only a single structural unit for determining the fully developed heat transfer coefficient without any empiricism. A universal correlation for the Nusselt number, which agrees well with available experimental data, has been established using the results obtained for a wide range of porosity, Prandtl and Reynolds numbers. © 2001 Elsevier Science Ltd. All rights reserved.

1. Introduction

There are certain situations where net heat transfer from one phase to another phase takes place in saturated porous media such that the assumption of local thermal equilibrium breaks down. The need for two-energy equation models (allowing two temperatures in two different phases) has long been recognized [1].

When there is a significant heat generation occurring in any one of the two phases (solid or fluid), the temperatures in the two phases are no longer identical [2]. The assumption of local thermal equilibrium must be discarded when we analyze the entrance region of packed column where a hot gas flows at a high speed. Many of unsteady problems associated with saturated porous media need treatments, which allow heat transfer from one phase to another. When the temperature at the bounding surface changes significantly with respect to time, and when solid and fluid phases have significantly different heat capacities and thermal conductivities, the local rate of change of temperature for one phase differs significantly from that for the other phase [3].

Moreover, Quintard [4] argues that assessing the validity of the assumption of local thermal equilibrium is not a simple task, since the temperature difference between the two phases cannot easily be estimated, and suggests that the use of a two-energy equation model is a possible solution to the problem. Numerous other physical situations where local thermal equilibrium fails are cited by Quintard and Whitaker [5].

Two energy equation models have been introduced heuristically in the literature [6]. These heuristic model equations fit in the following form:

$$\varepsilon\rho_{\mathrm{f}}C_{\mathrm{p_f}}\left[\frac{\partial\langle T\rangle^{\mathrm{f}}}{\partial t}+\langle\vec{u}\rangle^{\mathrm{f}}\cdot\nabla\langle T\rangle^{\mathrm{f}}\right]=\nabla\cdot\bar{\bar{k}}^{\mathrm{f}}_{\mathrm{eff}}\cdot\nabla\langle T\rangle^{\mathrm{f}}+h_{\mathrm{sf}}a_{\mathrm{sf}}\left(\langle T\rangle^{\mathrm{s}}-\langle T\rangle^{\mathrm{f}}\right),\tag{1}$$

$$(1-\varepsilon)\rho_{\mathrm{s}}C_{\mathrm{s}}\frac{\partial\langle T\rangle^{\mathrm{s}}}{\partial t}=\nabla\cdot\bar{\bar{k}}^{\mathrm{s}}_{\mathrm{eff}}\cdot\nabla\langle T\rangle^{\mathrm{s}}-h_{\mathrm{sf}}a_{\mathrm{sf}}\left(\langle T\rangle^{\mathrm{s}}-\langle T\rangle^{\mathrm{f}}\right),\tag{2}$$

where the subscripts (and superscripts) f and s denote fluid and solid phases, respectively. $\langle\vec{u}\rangle$ is the volume-averaged velocity (i.e., Darcian velocity), whereas $\langle T\rangle^{\mathrm{f}}$

* Corresponding author. Fax: +81-53-478-1049.

E-mail address: tmanaka@ipc.shizuoka.ac.jp (A. Nakayama).

0017-9310/01/$ - see front matter
PII: S0017-9310(00)00166-6

Nomenclature

$\vec{A}$	surface area vector
A_{int}	total interface between the fluid and solid
C_{p}	specific heat at constant pressure
C_{s}	specific heat of solid
D	size of square rod
H	size of structural unit
h_{sf}	interfacial convective heat transfer coefficient
u, v	microscopic velocity components in the x- and y-directions
T	microscopic temperature
p	microscopic pressure
k	thermal conductivity
Re	Reynolds number based on H and the macroscopically uniform velocity
Re_D	Reynolds number based on D and the macroscopically uniform velocity
Pe	Peclet number based on H and the macroscopically uniform velocity
Pe_D	Peclet number based on D and the macroscopically uniform velocity
V	elementary representative volume
x, y	Cartesian coordinates
ε	porosity
v	kinematic viscosity
ρ	density

Subscripts and superscripts

eff	effective
dis	dispersion
f	fluid
s	solid
tor	tortuosity

Special symbols

$\langle\ \rangle$	volume-average
$\langle\ \rangle^{\mathrm{f,s}}$	intrinsic average

and $\langle T\rangle^{\mathrm{s}}$ denote the intrinsically averaged temperature of fluid phase and that of solid phase, respectively, such that $\langle T\rangle^{\mathrm{f}} = \langle T\rangle^{\mathrm{s}}$ under local thermal equilibrium. Moreover, ε, $\bar{\bar{k}}_{\mathrm{eff}}$, a_{sf} and h_{sf} are the porosity, effective thermal conductivity tensor, specific surface area and interfacial convective heat transfer coefficient, respectively. In the two-equation model, the interfacial heat transfer coefficient h_{sf} and two thermal conductivity tensors $\bar{\bar{k}}^{\mathrm{f}}_{\mathrm{eff}}$ and $\bar{\bar{k}}^{\mathrm{s}}_{\mathrm{eff}}$ need to be determined. Quintard and Whitaker [5] obtained somewhat different form of the equations from the point of view of the volume-averaging theory. The major difference between their form and the foregoing heuristic form is the appearance of additional coupling terms. They claim that these coupling terms are not necessarily negligible. Although their model appears to be more general than the classical one, it requires four thermal conductivity tensors in addition to the interfacial convective heat transfer coefficient. Some theoretical attempts of determining these transport coefficients have been made by Quintard and Whitaker [5]. However, the unknown transport coefficients as well as part of the formulation itself make it difficult and awkward for simulating practical applications [7]. Viskanta [8] foresees that the classical form described by Eqs. (1) and (2) will continue to be used with empirical transport coefficients.

In this paper, we shall propose a numerical procedure to determine the macroscopic transport coefficients such as h_{sf} purely from a theoretical basis without any empiricism. Upon extending the numerical procedure for thermal equilibrium, developed by Nakayama et al. [9] and Kuwahara et al. [10], to the case of non-thermal equilibrium, we will conduct numerical experiments for a wide range of porosity, Prandtl and Reynolds numbers. Noting the similarity of fully developed temperature profiles, we shall use only a single structural unit to simulate a porous medium, and determine the interfacial heat transfer coefficient for the asymptotic case in which the conductivity of solid phase is infinite.

2. Volume-averaged energy equations and expressions for transport coefficients

Let us compare the foregoing Eqs. (1) and (2) of the classical model with the intrinsic volume-averaged equations obtained by integrating the individual energy equations over a representative elementary volume V. (Note that $V^{1/3}$ must be much smaller than a macroscopic characteristic length, but at the same time, much larger than a pore size.) Following Cheng [11] and Nakayama [12], we obtain the following macroscopic energy equations for the two individual phases:

$$\varepsilon\rho_{\mathrm{f}}C_{\mathrm{p_f}}\left[\frac{\partial\langle T\rangle^{\mathrm{f}}}{\partial t}+\langle\vec{u}\rangle^{\mathrm{f}}\cdot\nabla\langle T\rangle^{\mathrm{f}}\right] = \nabla\cdot\left[\varepsilon k_{\mathrm{f}}\nabla\langle T\rangle^{\mathrm{f}}+\frac{1}{V}\int_{A_{\mathrm{int}}}k_{\mathrm{f}}T\,\mathrm{d}\vec{A}-\rho_{\mathrm{f}}C_{\mathrm{p_f}}\langle T'\vec{u}'\rangle\right] + \frac{1}{V}\int_{A_{\mathrm{int}}}k_{\mathrm{f}}\nabla T\cdot\mathrm{d}\vec{A}, \tag{3}$$

$$(1-\varepsilon)\rho_{\mathrm{s}}C_{\mathrm{s}}\frac{\partial\langle T\rangle^{\mathrm{s}}}{\partial t} = \nabla\cdot\left[(1-\varepsilon)k_{\mathrm{s}}\nabla\langle T\rangle^{\mathrm{s}}-\frac{1}{V}\int_{A_{\mathrm{int}}}k_{\mathrm{s}}T\,\mathrm{d}\vec{A}\right] - \frac{1}{V}\int_{A_{\mathrm{int}}}k_{\mathrm{f}}\nabla T\cdot\mathrm{d}\vec{A}, \tag{4}$$

where

$$\langle\phi\rangle \equiv \frac{1}{V}\int_{V_f} \phi \, dV = \varepsilon\langle\phi\rangle^f \tag{5a}$$

$$\phi' \equiv \phi - \langle\phi\rangle^f. \tag{5b}$$

A_{int} is the total interface between the fluid and solid, while $d\vec{A}$ is its vector element pointing outward from the fluid side to solid side. The continuity of heat flux at the interface is implemented in the above equation. The comparison of the volume-averaged Eqs. (3) and (4) against the heuristic Eqs. (1) and (2) reveals the following relationships:

$$\bar{\bar{k}}^f_{eff} \cdot \nabla\langle T\rangle^f \equiv \varepsilon k_f \nabla\langle T\rangle^f + \frac{1}{V}\int_{A_{int}} k_f T \, d\vec{A} - \rho_f C_{p_f}\langle T'\vec{u}'\rangle, \tag{6}$$

$$\bar{\bar{k}}^s_{eff} \cdot \nabla\langle T\rangle^s \equiv (1-\varepsilon)k_s \nabla\langle T\rangle^s - \frac{1}{V}\int_{A_{int}} k_s T \, d\vec{A}, \tag{7}$$

$$h_{sf} \equiv \frac{\frac{1}{V}\int_{A_{int}} k_f \nabla T \cdot d\vec{A}}{\left(\langle T\rangle^s - \langle T\rangle^f\right)}. \tag{8}$$

Shortly, we propose a numerical model describing a microscopic structure of porous medium, for which we shall carry out direct numerical (i.e., pore scale) computations using the first principles. By substituting the direct numerical results into the foregoing expressions, we can determine the effective thermal conductivity tensors and the interfacial heat transfer coefficient of interest.

In the previous numerical study of thermal dispersion, Kuwahara et al. [10,13] found that the thermal dispersion term $-\rho_f C_{pf}\langle T'\vec{u}'\rangle$ overwhelms the other two terms resulting from the molecular diffusion and tortuosity in Eq. (6), such that $\bar{\bar{k}}^f_{eff} = \varepsilon k_f \bar{\bar{I}} + \bar{\bar{k}}_{tor} + \bar{\bar{k}}_{dis} \approx \bar{\bar{k}}_{dis}$, as the pore Peclet number Pe_D becomes sufficiently large. They established the following correlations for the transverse and longitudinal components of the thermal dispersion tensor, which are valid for $Pe_D \geqslant 10$, $2 \leqslant k_s/k_f \leqslant 100$ and $0.36 \leqslant \varepsilon \leqslant 0.96$:

$$\frac{(k_{dis})_{xx}}{k_f} = 2.1\frac{Pe_D}{(1-\varepsilon)^{0.1}}, \quad \text{Longitudinal dispersion,} \tag{9a}$$

$$\frac{(k_{dis})_{yy}}{k_f} = 0.052(1-\varepsilon)^{1/2}Pe_D, \quad \text{Transverse dispersion.} \tag{9b}$$

The foregoing correlations obtained from the numerical experiments agree quite well with the experimental data reported by Fried and Combarnous [14]. In what follows, we shall consider a numerical model and solution procedure to determine the interfacial heat transfer coefficient, for which a great deal of uncertainty and inconsistency were found among the experimental data reported by a considerable number of sources [2]. No numerical experiments of this kind seem to have been reported elsewhere.

3. Numerical model and periodic boundary conditions

Fluid particles experience complex three-dimensional motions as passing through a microscopic porous structure. The macroscopic hydrodynamic and thermodynamic behavior of practical interest can be obtained from the direct application of the first principles to viscous flow and heat transfer at a pore scale. In reality, however, it is impossible to resolve the details of the flow and heat transfer fields within a real porous medium, even with a most powerful super-computer available today. Nakayama et al. [9] and Kuwahara et al. [10] modeled a porous medium in terms of obstacles arranged in a regular pattern, and solved the set of the microscopic governing equations, exploiting periodic boundary conditions.

Three-dimensional models are much more relevant than two-dimensional ones for simulating flows through porous media. However, such three-dimensional computations are extremely expensive and time-consuming, even using a periodic structural model. Fortunately, a series of our numerical investigations using both two- and three-dimensional models [15] reveal that the two-dimensional models lead to the expressions for the permeability almost identical to those obtained using the three-dimensional models. Furthermore, the thermal dispersion predicted using a two-dimensional model [10,13] is found very close to what has been experimentally observed. Yet, it is not clear how well the two-dimensional model performs for determining the interfacial convective heat transfer coefficient. Although there is a certain limitation to it, a two-dimensional model can be exploited to elucidate complex flow and heat transfer characteristics associated with a porous medium. We shall extend the numerical procedure based on a two-dimensional model to determine the interfacial convective heat transfer coefficient.

Let us consider a macroscopically uniform flow through an infinite number of square rods placed in a staggered fashion, as shown in Fig. 1. All square rods, which may be regarded as heat sinks (or sources), are isothermal and maintained at a constant temperature T_w, which is lower (or higher) than the bulk mean temperature of the flowing fluid. In other words, we consider an asymptotic case in which the thermal conductivity ratio k_s/k_f is infinitely large.

The representative elementary volume V, which should be smaller than a macroscopic characteristic

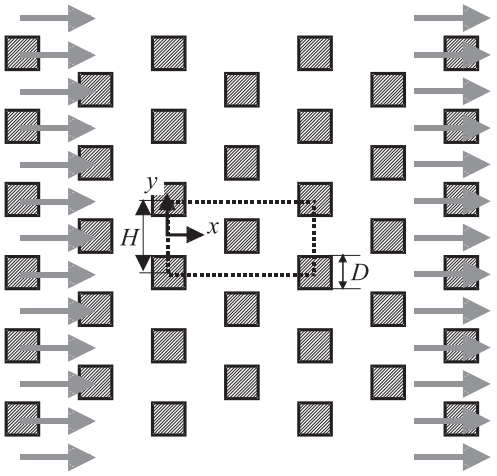

Fig. 1. Physical model and its coordinate system.

length, can be taken as $2H \times H$ for this periodic structure. Due to the periodicity of the model, only one structural unit as indicated by dashed lines in the figure may be taken as a calculation domain. The governing equations for the fluid phase are given as follows:

$$\nabla \cdot \vec{u} = 0, \tag{10}$$

$$(\nabla \cdot \vec{u})\vec{u} = -\frac{1}{\rho}\nabla p + \nu\nabla^2\vec{u}, \tag{11}$$

$$\rho_f C_{p_f} \nabla \cdot (\vec{u}T) = k_f \nabla^2 T. \tag{12}$$

At the periodically fully developed stage, the velocity distribution at the exit of the structural unit must be *identical* to that at the inlet, whereas the temperature profile at the exit must be *similar* to that at the inlet. (Note that the situation is analogous to the case of forced convection in a channel with isothermal walls, which will be considered shortly.) Thus, the boundary, compatibility and periodic constraints are given by

On the solid walls:

$$\vec{u} = \vec{0}, \tag{13a}$$

$$T = T_w. \tag{13b}$$

On the periodic boundaries:

$$\vec{u}|_{x=0} = \vec{u}|_{x=2H}, \tag{14}$$

$$\int_{-H/2}^{H/2} u\,\mathrm{d}y\bigg|_{x=0} = \int_{-h/2}^{H/2} u\,\mathrm{d}y\bigg|_{x=2H} = H\langle|\vec{u}|\rangle, \tag{15}$$

$$(T - T_w)|_{x=2H} = \tau(T - T_w)|_{x=0}, \tag{16}$$

where

$$\tau \equiv \frac{\int_{-H/2}^{H/2} u(T - T_w)\,\mathrm{d}y|_{x=2H}}{\int_{-H/2}^{H/2} u(T - T_w)\,\mathrm{d}y|_{x=0}} = \frac{(T_B - T_w)|_{x=2H}}{(T_B - T_w)|_{x=0}}. \tag{17}$$

$T_B(x)$ is the bulk mean temperature of the fluid. Computations can be made using the dimensionless equations based on the Darcian velocity $|\langle\vec{u}\rangle|$, the length of structural unit H and the temperature difference $(T_B(0) - T_w)$ as reference scales. For carrying out computations for a parametric study, it may be convenient to use the Reynolds number based on H as $Re = |\langle\vec{u}\rangle|H/\nu$, which is related to the Reynolds number based on D as $Re_D = |\langle\vec{u}\rangle|D/\nu = (1-\varepsilon)^{1/2}Re$, via $\varepsilon = 1 - (D/H)^2$.

4. Method of computation and preliminary numerical consideration

The governing equations are discretized by integrating them over a grid volume. SIMPLE algorithm for the pressure–velocity coupling, as proposed by Patankar and Spalding [16] is employed. Convergence is measured in terms of the maximum change in each variable during an iteration. The maximum change allowed for the convergence check is set to 10^{-5}, as the variables are normalized by appropriate references. A fully implicit scheme is adopted with the hybrid differencing scheme for the advection terms. Further details on this numerical procedure can be found in Patankar [17] and Nakayama [12].

All computations have been carried out for a one-structural unit $2H \times H$ using non-uniform grid arrangements with 90×45, to ensure that the results are independent of the grid system. The Reynolds number was varied from 10^{-2} to 10^3 and the porosity from 0.36 to 0.96, whereas the Prandtl number was varied from 10^{-2} to 10^2. All computations were performed using the computer system CONVEX 220 at Shizuoka University Computer Center.

Before carrying out numerical experiments to determine h_{sf}, the validity of the present numerical procedure based on the periodic boundary conditions must be substantiated. Thus, the preliminary computations have been conducted for forced convective flow in a channel, whose upper and lower wall surfaces are maintained at a constant temperature. We expect that the heat transfer coefficient approach its fully developed value, as the Graetz number becomes sufficiently large downstream.

Consider a short segment of an infinitely long channel, given by the length L and the height H, as shown in Fig. 2. Iterative calculations were carried out such that the resulting velocity and temperature fields satisfy the boundary conditions and periodic constraints given by Eqs. (13)–(17). (Note that the dimensionless velocity u^*

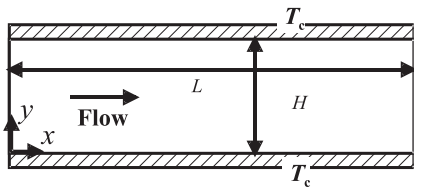

Fig. 2. Channel flow.

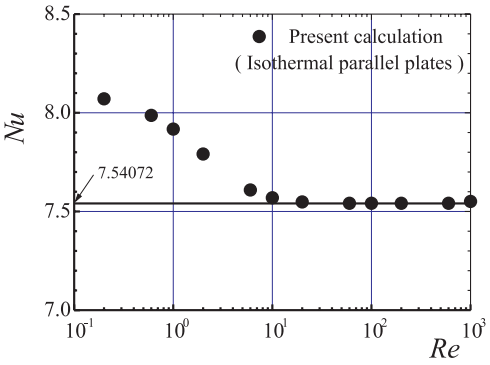

Fig. 3. Fully developed Nusselt number in a channel ($Pr = 1$).

and temperature T^* profiles at the inlet must be corrected iteratively such that $\int_{-1/2}^{1/2} u^* \, dy^* = \int_{-1/2}^{1/2} u^* T^* \, dy^* = 1$.) It can easily be shown that the unknown similarity parameter τ is uniquely related to the fully developed Nusselt number as

$$Nu \equiv \frac{h_{FD}(2H)}{k_f} = \frac{\rho_f C_{p_f} u_B H^2}{k_f L} \ln\left(\frac{1}{\tau}\right). \tag{18}$$

It has been confirmed that the velocity and temperature profiles become fully developed as convergence is achieved. In Fig. 3, the numerical results obtained by the present periodic procedure using the grid system (40×40) have been plotted in terms of the fully developed Nusselt number based on Eq. (18). As increasing the Reynolds (Graetz) number, the Nusselt number attaints its asymptotic value $Nu \to 7.54$ [18], which substantiates the validity of the present numerical procedure.

5. Results and discussion

The velocity and temperature fields obtained for three different Reynolds numbers are shown in Figs. 4 and 5, respectively. When the Reynolds number is low (say $Re = 1$), the velocity field around a rod (except front and rear stagnation regions) appears very much similar to what we observe in a channel, namely the parabolic profile. As increasing Re, recirculation bubbles expand further behind the rod. When the Reynolds

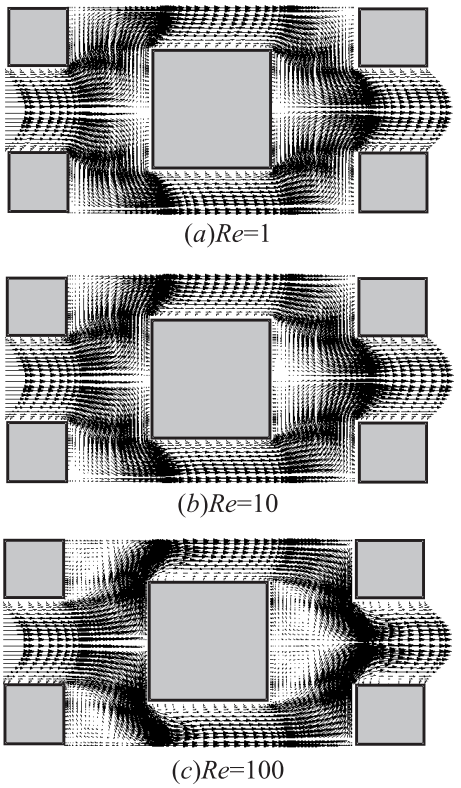

Fig. 4. Velocity vectors ($Pr = 1$).

number is sufficiently high, the thermal boundary layers cover around the rods as shown in Fig. 5(c), such that convective heat transfer overwhelms thermal diffusion.

The microscopic temperature results obtained with $Pr = 1$ for various values of Re and ε are processed using Eq. (19), and the resulting values of the interfacial convective heat transfer coefficient h_{sf} are plotted against Re in Fig. 6. The figure suggests that the lower and higher Reynolds number data follow two distinct limiting lines. The lower Reynolds number data stay constant for given porosity, whereas the high Reynolds number data vary in proportion to $Re^{0.6}$. The Reynolds number dependency is the same as what Wakao and Kaguei [2] observed as collecting and scrutinizing reliable experimental data on interfacial convective heat transfer coefficient.

Exhaustive computations were conducted to extract functional relationships for the interfacial convective heat transfer coefficient, assuming the following functional form:

$$\frac{h_{sf} D}{k_f} = a + b Re_D^m Pr^n, \tag{19}$$

which is in accord with the heuristic correlation of Wakao and Kaguei [2] for closely packed bed, of particle diameter D, namely

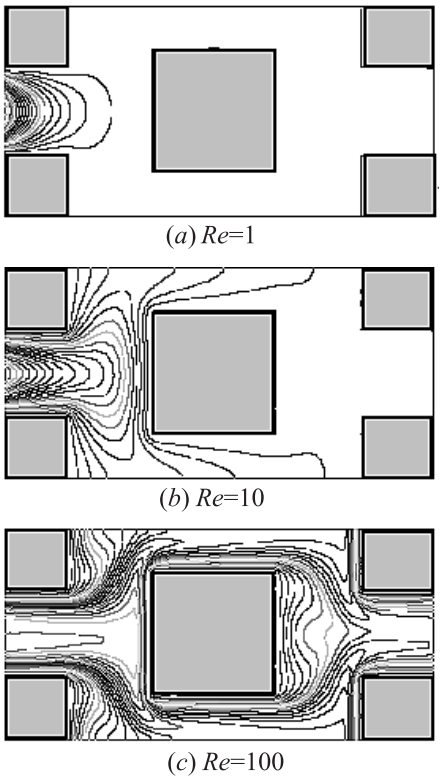

Fig. 5. Isotherms ($Pr = 1$).

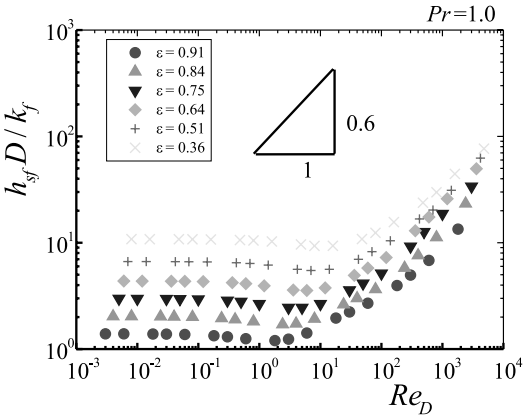

Fig. 6. Effect of Re_D on h_{sf} ($Pr = 1$).

$$\frac{h_{sf}D}{k_f} = 2 + 1.1Re_D^{0.6}Pr^{1/3}. \tag{20}$$

The coefficients a and b obtained for different ε are plotted in Fig. 7 with the abscissa variable $(1-\varepsilon)$ to investigate the porosity dependency. Another series of computations were carried out to investigate the effect of Pr as shown in Fig. 8 in which the exponent n can be

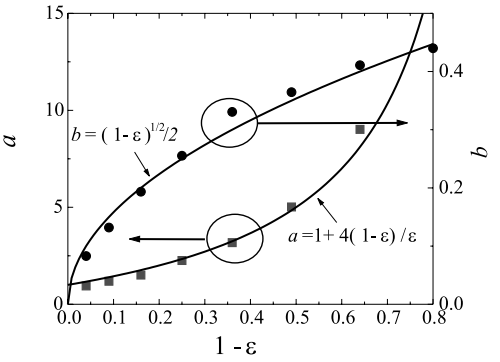

Fig. 7. Effect of porosity on intercept a ($Pr = 1$).

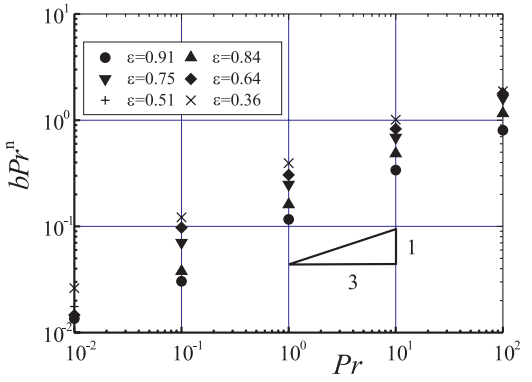

Fig. 8. Effect of Pr on coefficient.

found to be 1/3, in accord with the Wakao and Kaguei correlation. Thus, the following expression can be established from the numerical experiments based on the two-dimensional model:

$$\frac{h_{sf}D}{k_f} = \left(1 + \frac{4(1-\varepsilon)}{\varepsilon}\right) + \frac{1}{2}(1-\varepsilon)^{1/2}Re_D^{0.6}Pr^{1/3} \quad (0.2 < \varepsilon\ 0.9). \tag{21}$$

In Fig. 9, the foregoing expression for the interfacial convective heat transfer coefficient is compared against the experimental data for packed beds assembled by Wakao and Kaguei [2]. (Wakao and Kaguei assembled both steady and unsteady data together. But, our recent study based on unsteady numerical experiments suggests that a separate correlation should be established for correlating the unsteady data. Also note that Wakao and Kaguei had to correct some of the experimental data obtained neglecting the axial diffusion effects, so as to conform with the definition as given by Eq. (8).) The theoretical curves are generated from Eq. (21) with $\varepsilon = 0.2, 0.3$ and 0.4 and presented together in the figure. In the same figure, the heuristic expression proposed by Wakao and Kaguei is shown for reference, which is valid

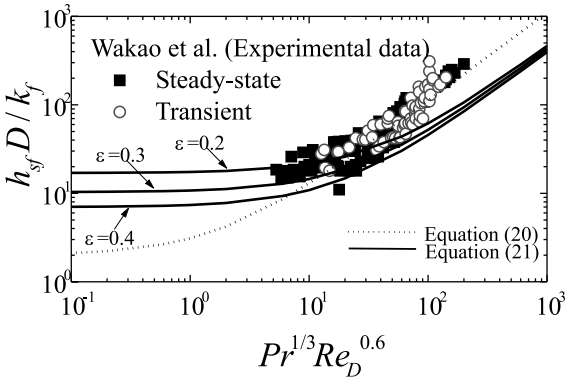

Fig. 9. Comparison of the prediction and experiment.

only for packed beds ($\varepsilon \approx 0.4$). Since we forced the flow to be steady, the heat transfer coefficient for the case in which vortex shedding takes place, may be underestimated to some extent. The agreement between the present correlation ($\varepsilon = 0.4$) and the experimental data can be regarded as reasonable, in light of the simplicity of the present periodic model.

6. Concluding remarks

The correlation for the interfacial convective heat transfer coefficient has been established from a series of numerical experiments based on a two-dimensional structural model of porous media. A macroscopically uniform flow through a periodic model of isothermal square rods was assumed, considering periodically fully developed velocity and temperature fields. Upon noting the similarity of the temperature profile, only a single structural unit has been taken for a calculation domain. Effects of the porosity, Reynolds and Prandtl numbers on the heat transfer coefficient have been elucidated. It has been found that the correlation established purely from a theoretical basis agrees well with available experimental data.

References

[1] T.E.W. Schumann, Heat transfer: liquid flowing through a porous prism, J. Franklin. Inst. 208 (1929) 405–416.

[2] N. Wakao, S. Kaguei, Heat and Mass Transfer in Packed Beds, Gorden and Breach, New York, 1982, pp. 243–295.

[3] M. Kaviany, Principles of Heat Transfer in Porous Media, second ed., Springer, New York, 1995, pp. 391–424.

[4] M. Quintard, Modelling local non-equilibrium heat transfer in porous media, Proc. 11th Int. Heat Transfer Conf. 1 (1998) 279–285.

[5] M. Quintard, S. Whitaker, One- and two-equation models for transient diffusion processes in two-phase systems, Adv. Heat Transfer 23 (1993) 369–464.

[6] E.U. Schlunder, Equivalence of one- and two-phase models for heat transfer processes in packed beds: one-dimensional theory, Chem. Eng. Sci. 30 (1975) 449–452.

[7] K. Vafai, A. Amiri, Non-Darcian effects in confined forced convective flows, in: D.B. Ingham, I. Pop, (Eds.), Transport Phenomena in Porous Media. Pergamon, Oxford, 1998, pp. 313–29.

[8] R. Viskanta, Modeling of transport phenomena in porous media using a two-energy equation model, Proc. ASME/JSME Thermal Eng. Conf. 3 (1995) 11–22.

[9] A. Nakayama, F. Kuwahara, Y. Kawamura, H. Koyama, Three-dimensional numerical simulation of flow through a microscopic porous structure, Proc. ASME/JSME Thermal Eng. Conf. 3 (1995) 313–318.

[10] F. Kuwahara, A. Nakayama, H. Koyama, A numerical study of thermal dispersion in porous media, J. Heat Transfer 118 (1996) 756–761.

[11] P. Cheng, Heat transfer in geothermal systems, Adv. Heat Transfer 14 (1978) 1–105.

[12] A. Nakayama, PC-aided numerical heat transfer and convective flow. CRC Press, Boca Raton, 1995, pp. 177–250.

[13] F. Kuwahara, A. Nakayama, Numerical determination of thermal dispersion coefficients using a periodic porous structure, J. Heat Transfer 121 (1999) 160–163.

[14] J.J. Fried, M.A. Combarnous, Dispersion in porous media, Adv. Hydrosci 7 (1971) 169–282.

[15] F. Kuwahara, A. Nakayama, H. Koyama, Numerical modelling of heat and fluid flow in a porous medium, Proc. 10th Int. Heat Transfer Conf. 5 (1994) 309–314.

[16] S.V. Patankar, D.B. Spalding, A calculation procedure for heat, mass and momentum transfer in three-dimensional parabolic flows, Int. J. Heat Mass Transfer 15 (1972) 1787–1806.

[17] S.V. Patankar, Numerical Heat Transfer and Fluid Flow. Hemisphere, Washington, DC, 1980.

[18] R.K. Shah, A.L. London, Laminar flow forced convection in ducts. in: Adv. Heat Transfer (Suppl. 1) Academic Press, New York, 1978.